Two-dimensional electron states bound to an off-plane donor in a magnetic field

2010 J. Phys.: Condens. Matter 22 125801

(http://iopscience.iop.org/0953-8984/22/12/125801)

J. Phys.: Condens. Matter **22** (2010) 125801 (8pp) doi:10.1088/0953-8984/22/12/125801

Two-dimensional electron states bound to an off-plane donor in a magnetic field

A Bruno-Alfonso[1], L Cândido[2,3] and G-Q Hai[2]

[1] Departamento de Matemática, Faculdade de Ciências, UNESP—Univ Estadual Paulista, 17033-360, Bauru, SP, Brazil
[2] Instituto de Física de São Carlos, Universidade de São Paulo, 13560-970, São Carlos, SP, Brazil
[3] Instituto de Física, Universidade Federal de Goiás, 74001-970, Goiânia, GO, Brazil

Received 9 November 2009, in final form 14 February 2010
Published 11 March 2010
Online at stacks.iop.org/JPhysCM/22/125801

Abstract
The states of an electron confined in a two-dimensional (2D) plane and bound to an off-plane donor impurity center, in the presence of a magnetic field, are investigated. The energy levels of the ground state and the first three excited states are calculated variationally. The binding energy and the mean orbital radius of these states are obtained as a function of the donor center position and the magnetic field strength. The limiting cases are discussed for an in-plane donor impurity (i.e. a 2D hydrogen atom) as well as for the donor center far away from the 2D plane in strong magnetic fields, which corresponds to a 2D harmonic oscillator.

(Some figures in this article are in colour only in the electronic version)

1. Introduction

Since the quantum states of a dopant impurity in semiconductor Si were proposed for implementing a quantum computer [1], the study of shallow donor impurities near semiconductor surfaces and interfaces has gained new interest. Recent progress in dopant engineering and coherent control of dopant states, together with the amazing advances in Si technology, have accelerated the realization of devices based on the quantum functionality of single dopants [2, 3]. Basic elements such as P and As are promising candidates, as dopants, in these nanometer-scale quantum electronic devices. A recent experiment [4] has proven that it is possible to manipulate the states of an individual electron bound to a single dopant atom in a silicon field-effect transistor. The gate potential of the transistor was successfully used to control a single electron state between the core potential of its donor and a nearby quantum well (quantum dot) at the Si/oxide interface.

Shallow donors have been extensively studied in bulk and low-dimensional semiconductor systems, such as quantum wells and superlattices [5–8]. However, the new projected devices based on the quantum functionality of single dopants have stimulated much theoretical studies and numerical simulations on the quantum states of donors localized near a semiconductor surface or interface. In such structures, the quantum confinement potential of the heterostructure together with the donor Coulomb potential determine the bound electron states. An electric gate or an external magnetic field can be used to control and manipulate the electronic states to realize the operation of the devices. The ground state of a donor localized near a semiconductor/insulator/metal interface was recently investigated by using the finite element technique [9, 10], the variational approach [2, 9] and the quantum Monte Carlo simulation [11]. The effects of the gate potential, the screening of the metallic gate, the finite thickness of the insulator layer between the semiconductor and the gate, as well as the image charge on the impurity potential and the donor states, were investigated [9, 10].

In [2], Calderon *et al* studied the ground state energy of a donor localized in Si near an interface with a thick insulating layer in applied electric and magnetic fields perpendicular to the interface, taking into account the charge images of the impurity and the electron. They showed the existence of a well-defined interface state where the electron remains bound to its donor and localized in the semiconductor/insulator interface. The transition processes of the donor electron 'shuttling' between its parent donor state to the interface state were investigated. The energy spectrum of a donor near the semiconductor/insulator/metal interface was recently investigated in [9, 10]. In these studies, the effect of the finite thickness of the insulator layer and the importance of the screening effect of the metallic gate on the impurity states that are localized near the semiconductor/insulator interface were investigated. The effect of an electric field moving the

electron away from the donor site to the interface was also studied. It was shown that the screening of the metallic gate leads to a considerable lowering of the energy levels, especially when the impurity is located very near the interface. There are interesting limiting cases in the above studied systems. When the donor center is far away from the interface, the donor states approach the well-known three-dimensional (3D) magnetodonor states. In the opposite case, when the donor center is localized in the interface, the electron is confined in a (quasi-) two-dimensional quantum well. This is also an extensively studied problem over the last few decades and is well understood. However, in a strong (intermediate) positive gate potential for intermediate (large) values of the distance between the donor and the interface, the electron can be completely confined in the interfacial potential well and is still bound to the donor center. This is an interesting situation where the electron states are of a two-dimensional characteristic but are bound to an off-plane remote donor center in the third dimension.

In this work, we study the quantum states of an electron confined in a two-dimensional (2D) plane and bound to an off-plane shallow donor center in the presence of an external magnetic field. This is a simplified model for a donor localized near a semiconductor/insulator interface of intermediate (large) values of the distance between the donor and the interface subjected to a strong (intermediate) positive gate potential. It also corresponds to a system where the electron confined at the semiconductor/insulator interface is bound to a charge center localized in the insulator layer. Such a situation also happens when a donor impurity lies in the barrier material of a quantum well heterostructure, namely the so-called barrier neutral magnetodonor (D^0). In all these cases, the electron is subjected to both the Coulomb potential of the donor core and the quantum well confinement at the interface. In our present model, we simplify the quantum confinement at an interface being of zero thickness. The electron is confined completely in a 2D plane. We will also disregard the charge images of the impurity and the electron. In general, a finite thickness of the confinement potential in a quasi-2D system can reduce the binding energies of the localized states [8]. The charge images of the impurity and the electron and the screening of the metallic gate leads to a lowering of the energy levels [2, 9].

On the other hand, the 2D hydrogen atom is the limiting case of our problem as the donor center approaches the plane containing the electron. The 2D hydrogen atom, which originated as a purely theoretical construction [12–15], has been an interesting subject of study in the last two decades [16–20]. These studies have been motivated by the experimental realization of confined shallow donor impurities and excitons in quasi-2D quantum well structures. The energy levels and the orbitals [19, 20] of the 2D hydrogen atom, the properties in magnetic fields [19, 21], the dynamical symmetries [16–18], as well as the effects of the Rashba spin–orbital coupling [22], have been studied. The investigation of the 2D electronic states bound to an off-plane donor in the presence of a magnetic field is strongly motivated by the technological development and, naturally, has become the next step forward. Certainly, a full knowledge of the 2D states of an off-plane shallow donor is helpful for a better understanding of the physics of single dopants localized near an interface.

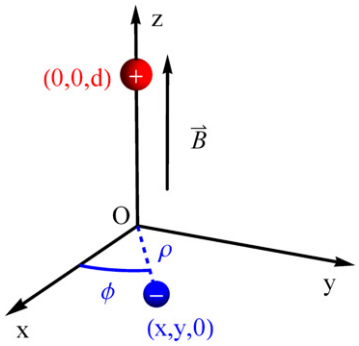

Figure 1. Pictorial view of the electron confined in the xy plane interacting with a positive charge at the z axis and subject to a magnetic field applied along this axis.

This paper is organized as follows. We present our theoretical model and the variational approach in section 2. In section 3, we discuss the numerical results of our calculations. The energy levels and the mean orbital radii of the ground state 1s and the excited states $2p^{\pm}$ and 2s of the hydrogenic donor are given as a function of the off-plane distance and the magnetic field strength. The conclusions are presented in section 4. The interaction matrix elements are given in the appendix.

2. The off-plane hydrogenic donor states

We consider an electron moving on the xy plane and bound to an off-plane positive charge, placed at the z axis (see figure 1). The impurity position is $(0, 0, d)$, where d is the distance from the 2D plane containing the electron to the charge center of the donor impurity (the donor–plane distance). An external uniform magnetic field of strength B is applied along the z axis. We express the length and energy in units of the effective Bohr radius a_B^* and the effective Rydberg R_y^*, respectively. As usual, the dimensionless parameter $\gamma = (a_B^*/\lambda)^2$ is introduced as a measure of the magnetic field strength, where $\lambda = \sqrt{(\hbar/eB)}$ is the Landau radius. In GaAs, the effective mass is $m^* = 0.067m_0$, where m_0 is the bare electron mass and the static dielectric permittivity is $\epsilon = 12.5$. Hence, $a_B^* = 98.7$ Å, $R_y^* = 5.83$ meV and $\gamma = 1$ corresponds to a magnetic field of $B = 6.75$ T. Instead, in a silicon-based structure grown along the (001) direction, the in-plane mass is $m^* = 0.190m_0$ and $\epsilon = 11.9$. Correspondingly, $a_B^* = 33$ Å, $R_y^* = 18.3$ meV and $\gamma = 1$ is for $B = 59.9$ T.

The Schrödinger equation of this impurity is given by

$$\hat{H}\Psi(\rho, \phi) = E\Psi(\rho, \phi). \tag{1}$$

By choosing the vector potential of the magnetic field in the symmetric gauge, the Hamiltonian operator takes the following form:

$$\hat{H} = -\frac{1}{\rho}\frac{\partial}{\partial\rho}\left(\rho\frac{\partial}{\partial\rho}\right) - \frac{1}{\rho^2}\frac{\partial^2}{\partial\phi^2} - i\gamma\frac{\partial}{\partial\phi} + \gamma^2\frac{\rho^2}{4} - \frac{2}{\sqrt{\rho^2 + d^2}}, \tag{2}$$

where ρ and ϕ are the usual polar coordinates.

According to the axial symmetry, the eigenfunctions of $\hat{H}$ are of well-defined angular momentum along the field direction. Namely, the eigenfunctions can be written as

$$\Psi_m(\rho,\phi) = \frac{e^{im\phi}}{\sqrt{2\pi}}\psi_m(\rho), \tag{3}$$

where m is an integer number and $\psi_m(\rho)$ satisfies the following equation:

$$(\hat{H}_\perp^{(m)} + V(\rho))\psi_m(\rho) = E_m\psi_m(\rho), \tag{4}$$

with

$$\hat{H}_\perp^{(m)} = -\frac{1}{\rho}\frac{d}{d\rho}\left(\rho\frac{d}{d\rho}\right) + \frac{m^2}{\rho^2} + \gamma m + \frac{\gamma^2\rho^2}{4} \tag{5}$$

and

$$V(\rho) = -\frac{2}{\sqrt{\rho^2+d^2}}. \tag{6}$$

For $d = \gamma = 0$, we have an in-plane impurity in the absence of magnetic field, i.e. the 2D hydrogen atom. In this case, the eigenenergies of (5) are given by

$$E_{\nu,m} = -\frac{1}{(\nu+|m|+\frac{1}{2})^2} = -\frac{1}{\rho_{\nu,m}^2}, \tag{7}$$

where $\nu = 0, 1, 2, \ldots$ and $\rho_{\nu,m} = \nu + |m| + \frac{1}{2}$. The corresponding eigenfunctions are

$$\psi_{\nu,m}(\rho) = \sqrt{\frac{2\nu!}{(\nu+2|m|)!}}\frac{(2\rho)^{|m|}e^{-\rho/\rho_{\nu,m}}}{\rho_{\nu,m}^{3/2+|m|}}L_\nu^{(2|m|)}\left(\frac{2\rho}{\rho_{\nu,m}}\right), \tag{8}$$

where $L_\nu^{(m)}(x)$ is the associate Laguerre polynomial. From (7), the energy of the ground state 1s ($\nu = 0, m = 0$) is $E_{1s} = -4$. The lowest excited states $2p^\pm$ ($\nu = 0, m = \pm 1$) and 2s ($\nu = 1, m = 0$) are threefold-degenerate, with $E_{2p^\pm} = E_{2s} = -4/9$. The mean orbital radius, defined by $\langle\rho\rangle_{\nu,m} = \langle\psi_{\nu,m}(\rho)|\rho|\psi_{\nu,m}(\rho)\rangle$, takes the following values for the above states: $\langle\rho\rangle_{1s} = 0.5$, $\langle\rho\rangle_{2p^\pm} = 3.0$ and $\langle\rho\rangle_{2s} = 3.5$.

When $d \gg 1$ and $\gamma \gg 1$, i.e. in the case of a donor center far away from the 2D plane and subject to a strong magnetic field, the electron localizes within a small region around the projection of the donor center position on the 2D plane. Accordingly, the donor potential can be approximated as

$$V(\rho) \approx -\frac{2}{d} + \frac{\rho^2}{d^3}. \tag{9}$$

The problem is thus reduced to a 2D oscillator in the presence of a magnetic field and the solutions are the well-known Fock–Darwin states [23, 24]. Namely, the eigenenergy of (4) with the potential (9) has the form

$$E_{\nu,m} = -\frac{2}{d} + m\gamma + (2\nu+|m|+1)\alpha, \tag{10}$$

where $\alpha = (\gamma^2 + 4/d^3)^{1/2}$, and the eigenfunction is given by

$$\psi_{\nu,m}(\rho) = \sqrt{\frac{2\nu!}{(\nu+|m|)!}}\left(\frac{\alpha}{2}\right)^{(|m|+1)/2} \times \rho^{|m|}e^{-\alpha\rho^2/4}L_\nu^{(|m|)}\left(\frac{\alpha\rho^2}{2}\right). \tag{11}$$

In the limit $d \to \infty$, $E_{\nu,m}$ is given by $(2N+1)\gamma$ with $N = \nu + (m+|m|)/2$, which is the Nth Landau level. Therefore, each bound state (ν, m) is associated with a certain Landau level. The corresponding binding energy can be defined as

$$E_B(\nu,m) = (2N+1)\gamma - E_{\nu,m}. \tag{12}$$

In particular, for $d \gg 1$, we obtain

$$E_B(\nu,m) \approx \frac{2}{d} - (2\nu+|m|+1)(\alpha-\gamma). \tag{13}$$

The mean radius of an impurity state in this limit is given by

$$\langle\rho\rangle_{\nu,m} = q_{\nu,m}\sqrt{\frac{\pi}{2\alpha}}, \tag{14}$$

where, for the ground and first excited states, $q_{0,0} = 1$, $q_{0,\pm1} = 3/2$ and $q_{1,0} = 7/4$.

In general, there are no analytical solutions available for (4). We solve this equation variationally by using the following trial wavefunction:

$$\psi_m(\rho) = \sum_n c_n^{(m)}R_{n,m}(\rho), \tag{15}$$

with

$$R_{n,m}(\rho) = \frac{1}{b}r_{n,m}\left(\frac{\rho}{b}\right), \tag{16}$$

and

$$r_{n,m}(x) = \sqrt{\frac{n!}{(n+|m|)!}}\left(\frac{x}{\sqrt{2}}\right)^{|m|}e^{-\frac{x^2}{4}}L_n^{(|m|)}\left(\frac{x^2}{2}\right), \tag{17}$$

where b is a variational parameter. In the numerical calculations, different variational parameters can be used for the different donor states. This point will be discussed in detail in section 3.

The coefficients $c_n^{(m)}$ in (15) satisfy the eigenvalue problem

$$\sum_{n'}(H_{\perp,n,n'}^{(m)} + V_{n,n'}^{(m)})c_{n'}^{(m)} = E_m c_n^{(m)}, \tag{18}$$

where

$$H_{\perp,n,n'}^{(m)} = \langle R_{n,m}(\rho)|\hat{H}_m^\perp|R_{n',m}(\rho)\rangle_\rho = \left(m\gamma + \frac{2n+|m|+1}{b^2}\right)\delta_{n,n'} + \frac{1}{4}\left(\gamma^2b^2 - \frac{1}{b^2}\right)Y_{n,n'}^{(|m|)}, \tag{19}$$

with

$$Y_{n,n'}^{(m)} = \int_0^{+\infty} x^3 r_{n,m}(x)r_{n',m}(x)\,dx = 2\big[(2n+m+1)\delta_{n,n'} - \sqrt{n'(n'+m)}\delta_{n+1,n'} - \sqrt{n(n+m)}\delta_{n,n'+1}\big]. \tag{20}$$

The matrix elements of the Coulomb term are given by

$$V_{n,n'}^{(m)} = -2\int_0^{+\infty}\frac{\rho}{\sqrt{\rho^2+d^2}}R_{n,m}(\rho)R_{n',m}(\rho)\,d\rho. \tag{21}$$

The calculation of this integral can be found in the appendix.

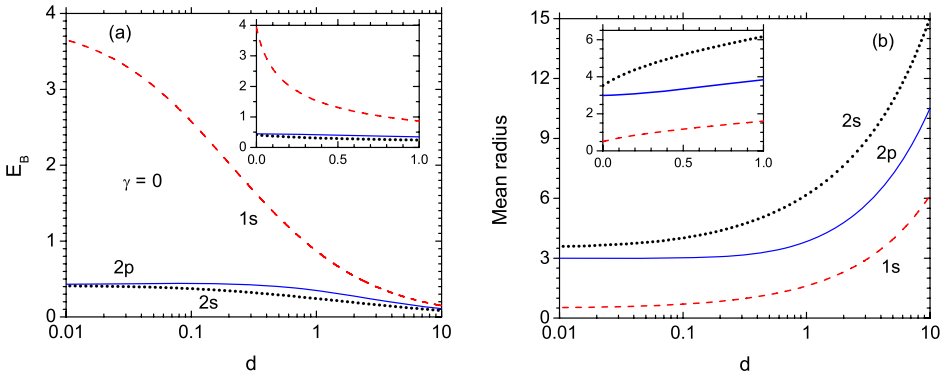

Figure 2. Semi-log plot of (a) the binding energy, E_B, and (b) the mean orbital radius of the 1s (dashed line), 2s (dotted line) and $2p^{\pm}$ (solid line) states as a function of the donor–plane distance d in the absence of magnetic field ($\gamma = 0$). The insets partially show the same data, but in the linear scale.

The coefficients $c_n^{(\nu,m)}$ (where ν is the index for the νth eigenvalue $E_{\nu,m}$ for a certain m) form the orthonormalized eigenvectors of the matrix $H^{(m)} = H_{\perp}^{(m)} + V^{(m)}$, which is real and symmetric. This leads to the orthonormalization of the eigenfunctions defined by (4) due to

$$\langle\psi_{\nu,m}(\rho)|\psi_{\nu',m}(\rho)\rangle_\rho = \sum_n c_n^{(\nu,m)} c_n^{(\nu',m)} = \delta_{\nu,\nu'}. \tag{22}$$

It is worth noting that we need not solve the numerical problem for $m > 0$. As a matter of fact, $E_{\nu,|m|} = E_{\nu,-|m|} + 2|m|\gamma$ and $\psi_{\nu,|m|}(\rho) = \psi_{\nu,-|m|}(\rho)$.

We also determine the mean radius of the orbital (ν, m) in the plane by the following expression:

$$\langle\rho\rangle_{\nu,m} = \langle\psi_{\nu,m}(\rho)|\rho|\psi_{\nu,m}(\rho)\rangle_\rho = b\sum_{n,n'} c_n^{(\nu,m)} c_{n'}^{(\nu,m)} X_{n,n'}^{(|m|)}, \tag{23}$$

where

$$X_{n,n'}^{(m)} = \int_0^{+\infty} x^2 r_{n,m}(x) r_{n',m}(x)\,\mathrm{d}x. \tag{24}$$

The value of this integral is given in the appendix.

3. Numerical results and discussions

We have calculated numerically the ground state 1s ($\nu = 0, m = 0$) and three excited states $2p^{\pm}$ ($\nu = 0, m = \pm 1$) and 2s ($\nu = 1, m = 0$) of a donor in the considered system. The energy level $E_{\nu,m}$ and the mean orbital radius of these states were obtained as a function of the donor–plane distance and the magnetic field strength. According to (12), for the 1s and $2p^-$ (2s and $2p^+$) states, the binding energy is $E_B(\nu, m) = \gamma - E_{\nu,m}$ ($E_B(\nu, m) = 3\gamma - E_{\nu,m}$). This is because these donor levels are associated with the zeroth and first Landau levels, with energies γ and 3γ, respectively.

In our variational calculation, we have used 13 basis functions, by taking $n = 0, 1, \ldots, 12$ for each m and ν. In the numerical calculations, we have tested firstly our trial wavefunctions for the ground state 1s and the excited states $2p^{\pm}$ by increasing the basis functions and comparing the obtained results of the energy levels and the mean orbital radii at $d = 0$ and $\gamma = 0$ to their exact values. Because the states with different m values are orthogonal automatically, the lowest energy level ($\nu = 0$) for $m = 0$ is the ground state 1s and the lowest energy level for $m = \pm 1$ is the $2p^{\pm}$ state. It is found that, by using up to 13 basis functions, we can obtain reasonably good accuracy for the energy levels and the mean orbital radii of these donor states. For $d = 0$ and $\gamma = 0$, the obtained energies of the 1s and $2p^{\pm}$ states are $E_{1s} = -3.9374$ and $E_{2p^{\pm}} = -0.4436$. In comparison with their exact energy $E_{1s} = -4$ and $E_{2p^{\pm}} = -4/9 = -0.4444$, the errors are 1.6% and 0.19%, respectively. The obtained mean orbital radii are $\langle\rho\rangle_{1s} = 0.4931$ and $\langle\rho\rangle_{2p^{\pm}} = 2.9906$, which are 1.4% and 0.32% smaller than the exact values $\langle\rho\rangle_{1s} = 0.5$ and $\langle\rho\rangle_{2p^{\pm}} = 3.0$, respectively. We also notice that these errors decrease rapidly with increasing the donor–plane distance d and/or magnetic field γ. From a detailed comparison of the variational calculations with the analytical results at the end of this section, we can see that, at $d = 5$ and $\gamma = 5$, the differences for these energy levels are less than 0.13% and those for the mean orbital radii are less than 0.003%. We also notice that, with increasing the basis functions further, the lowest energy level around its minimum is almost flat over a wide range of the parameter b, which hardly affects the energy level. On the other hand, a very large basis of radial functions would introduce extra numerical errors.

For the 1s and $2p^{\pm}$ states, the optimal value of the variational parameter b is determined by minimizing the lowest eigenvalue of $H^{(0)}$ and $H^{(1)}$, respectively. The energy of the 2s state may be estimated as the second eigenvalue of $H^{(0)}$ with the same variational parameter b used for the 1s level. Instead, we follow the procedure which was successfully used by Faulkner [25] to calculate the donor states in Si and Ge. An additional optimization is performed so that the second eigenvalue of $H^{(0)}$ is minimized as a function of b. Although this approach does not guarantee the orthogonality of the 1s and 2s states, it lowers the energy and improves the mean orbital radius of the state.

Figure 2 presents the numerical results for an off-plane donor in the absence of magnetic field ($\gamma = 0$). In this case, the $2p^{\pm}$ states are degenerate. The binding energy and the mean orbital radius of the 1s (dashed line), 2s (dotted line) and 2p (solid line) states are plotted as a function of the distance d

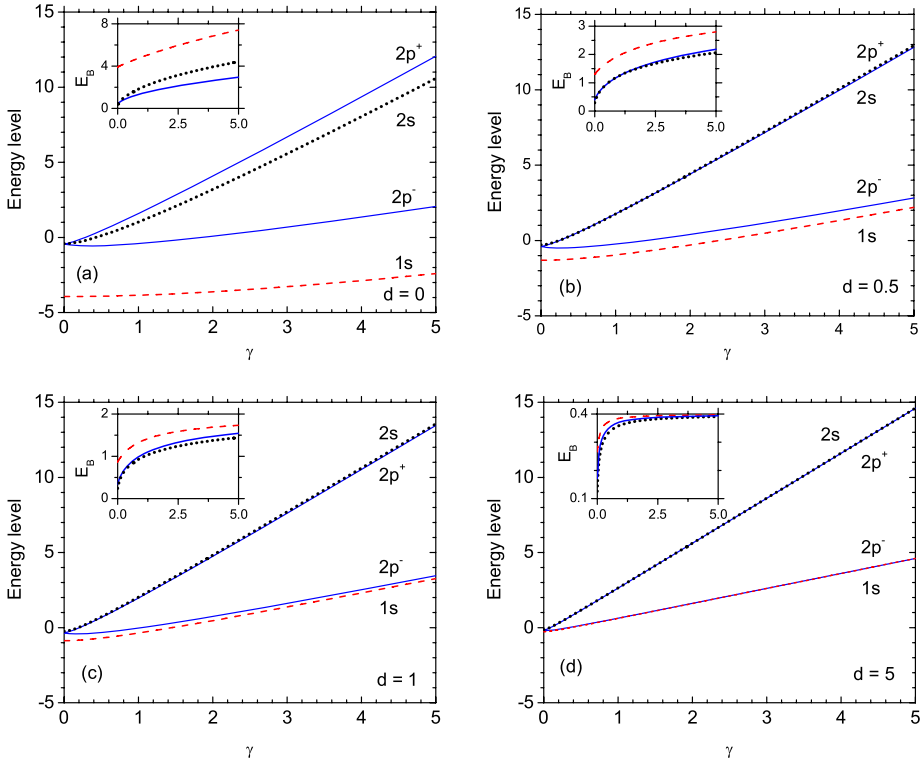

Figure 3. The energy levels of the 1s (dashed line), 2s (dotted line) and $2p^{\pm}$ (solid line) states as a function of the magnetic field strength, γ, for different values of the donor–plane distance: (a) $d = 0$, (b) $d = 0.5$, (c) $d = 1$ and (d) $d = 5$. The insets show the corresponding binding energies.

from the donor center to the 2D plane. The main panels are semi-log plots for $0.01 \leqslant d \leqslant 10$, while the insets are linear plots for $0 \leqslant d \leqslant 1$.

Figure 2(a) shows that the binding energy decreases as d increases. This is because the electron–impurity Coulomb interaction becomes weak as the distance between them increases. The binding energy of the ground state 1s depends strongly on the position of the donor center. A small displacement of the donor center from the 2D plane (a few tenths of the effective Bohr radius) leads to a significant decrease of the binding energy of the ground state. More exactly, $E_{\rm B}(1{\rm s}) = 3.71$, 2.58 and 2.03 for $d = 0.01$, 0.1 and 0.2, respectively. We note that, at $d = 0.2$, $E_{\rm B}(1{\rm s})$ is almost half of its value at $d = 0$.

Regarding the excited states, the 2s and 2p states are degenerate at $d = 0$ with the same binding energy. Figure 2 shows that the 2s state is more sensitive to the position of the impurity center than the 2p state. On increasing d, the binding energy (the mean radius) of the 2s state decreases (increases) faster than that of the 2p state. This can be understood by analyzing the symmetry of the states. Because the probability density of an s state is of finite value at the origin of the 2D plane, while that of a p state has to vanish due to its symmetry, a small displacement of the impurity center from the 2D plane noticeably affects the electrostatic energy of the electron in the s state. In contrast, for a p state, the electrostatic energy is rather insensitive for small d. For the same reason, the mean radii of the 1s and 2s states show similar behavior and increase faster than that of the 2p state for $d < 1$. For $d > 1$, the mean orbital radii of the these bound states increase rapidly with increasing d because the electron becomes loosely bound to the impurity center.

Figure 3 shows the energy levels of the 1s (dashed line), 2s (dotted line) and $2p^{\pm}$ (solid line) states as a function of the magnetic field strength for different donor–plane distances (a) $d = 0$, (b) $d = 0.5$, (c) $d = 1.0$ and (d) $d = 5.0$. Notice that the energy difference between the $2p^{+}$ and $2p^{-}$ states is 2γ. This figure clearly indicates that the 1s and $2p^{-}$ (the 2s and $2p^{+}$) levels are associated with the zeroth (the first) Landau level. In fact, for a large value of γ and/or d, the impurity energy levels approach their associated Landau levels. In this way, the binding energies of the $2p^{+}$ and $2p^{-}$ are the same. Hence, only three lines are displayed in the insets. The solid line is for the $2p^{\pm}$ states. Figure 2 has already shown that, at zero magnetic field, the binding energies of the 1s, 2s and $2p^{\pm}$ states diminish when the impurity center is far away from the plane. Now, figure 3 shows that the same thing happens when an external magnetic field is applied. On the other hand, for an in-plane impurity, the energy difference between 2s and $2p^{+}$ levels increases on increasing the magnetic field strength (see figure 3(a)). The binding energy of the 2s state is larger than that of the $2p^{+}$ state in a magnetic field. For finite donor–plane distance, however, the binding energy of the $2p^{+}$ state can be larger, as shown in the figure. This means that the energy levels of the two states cross at finite γ and d. As these states are of different symmetries, such a crossing of the energy levels is allowed. The binding energy for $d \gg 1$ and $\gamma \gg 1$ can be estimated by equation (13). In figure 3, this

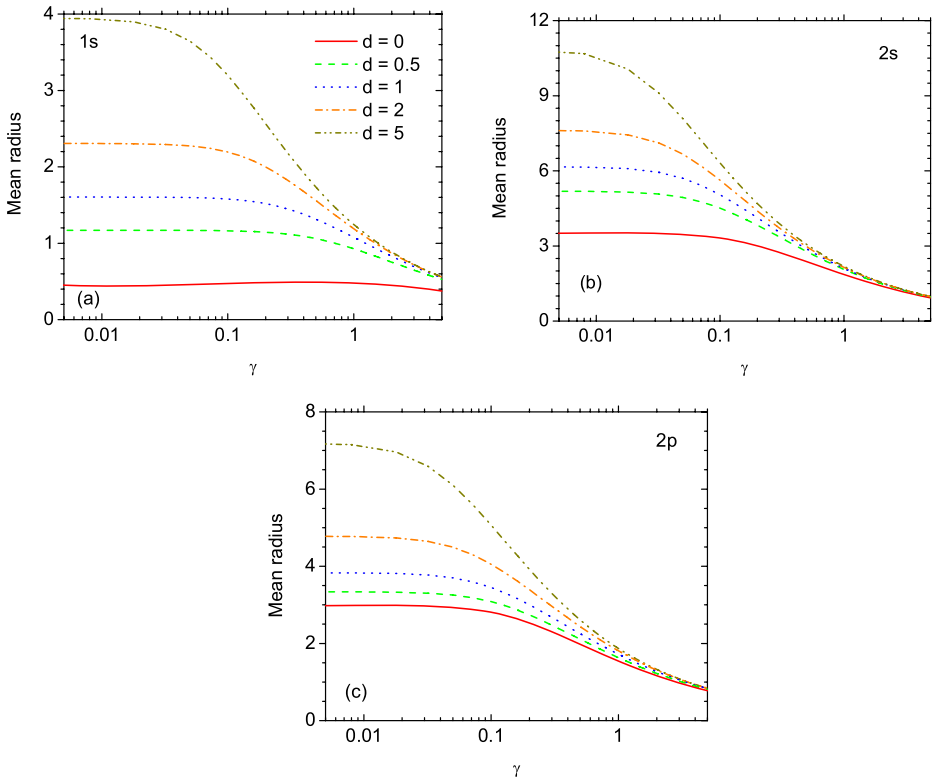

Figure 4. Mean orbital radius of the (a) 1s, (b) 2s and (c) 2p states as a function of the magnetic field strength for $d = 0$ (solid), 0.5 (dashed), 1 (dotted), 2 (dashed–dotted) and 5 (dashed–double-dotted).

corresponds to $d = 5$. For the 1s state, we obtain $E_B(1s) \approx 0.4 - g(\gamma)$, with $g(\gamma) = (\gamma^2 + 0.032)^{1/2} - \gamma$. When $\gamma = 5$, it gives $E_B(1s) \approx 0.396\,80$. This value is in good agreement with the value 0.396 88 given in figure 3(d). Moreover, for the excited states we obtain $E_B(2p^{\pm}) \approx 0.4 - 2g(\gamma)$ and $E_B(2s) \approx 0.4 - 3g(\gamma)$. For $\gamma = 5$, these expressions produce $E_B(2p^{\pm}) \approx 0.3936$ and $E_B(2s) \approx 0.3904$. Again, these values reproduce quite accurately the results shown in figure 3(d), i.e. $E_B(2p^{\pm}) \approx 0.3938$ and $E_B(2s) \approx 0.3909$.

Figure 4 displays the mean orbital radii of the (a) 1s (b) 2s and (c) 2p states as a function of the magnetic field strength for different donor–plane distances. It is seen that, at small γ, the mean orbital radius is quite large and depends strongly on the donor–plane distance. This is because the donor Coulomb potential dominates the radial confinement of the electron, which depends on the donor–plane distance. With increasing magnetic field, the orbitals of the bound states shrink. At large magnetic fields, equation (14) can be used to estimate the mean radius of the donor states provided that $d \gg 1$. In figure 4, this applies to the case of $d = 5$. For the 1s state this leads to $\langle\rho\rangle_{1s} \approx (\pi/2)^{1/2}(\gamma^2 + 4/d^3)^{-1/4}$. For $d = 5$ and $\gamma = 5$, it yields $\langle\rho\rangle_{1s} \approx 0.560\,32$. This is in good agreement with the value 0.560 33 according to figure 4(a). Furthermore, for the 2s and $2p^{\pm}$ states, equation (14) produces $\langle\rho\rangle_{2p^{\pm}} \approx 3/2\langle\rho\rangle_{1s}$ and $\langle\rho\rangle_{2s} \approx 7/4\langle\rho\rangle_{1s}$. For $d = 5$ and $\gamma = 5$, these simple formulae give $\langle\rho\rangle_{2p^{\pm}} \approx 0.840\,48$ and $\langle\rho\rangle_{2s} \approx 0.980\,56$. We find that these are close to the values given in figures 4(b) and (c) which are $\langle\rho\rangle_{2p^{\pm}} = 0.840\,50$ and $\langle\rho\rangle_{2s} = 0.980\,59$. Finally, in the limit $\gamma \gg 2/d^{3/2}$, the mean radius of the states is essentially independent of the donor–plane distance. This behavior is apparent in figure 4 and may be understood by the fact that the radial confinement of the electron is dominated by the magnetic field.

4. Conclusions

We have studied the two-dimensional states of an electron bound to an off-plane hydrogenic donor impurity in a magnetic field. The energy levels and wavefunctions were calculated variationally, and the corresponding binding energies and mean orbital radii of the 1s, $2p^{\pm}$ and 2s were determined. The binding energy increases on either decreasing the donor–plane distance or increasing the magnetic field strength. The opposite behavior was observed for the mean orbital radius of the bound states. In the limit of an in-plane impurity, our results correctly reproduce those of a 2D hydrogen atom. On the other hand, when the donor is far away from the electron plane in a strong magnetic field, our results were shown in good agreement with the approximation of a 2D harmonic oscillator subject to a magnetic field.

This study was motivated by recent advances in the experimental control of single electrons bound to shallow impurity states in semiconductor nanostructures and their potential applications in technology. Our study was focused on the situation where the electron is confined completely in the interface plane and bound to an off-plane donor center. We did not consider the control and manipulation of moving a single electron state between the core potential of its donor and the

nearby interface quantum well. In fact, we presented numerical results of the energy levels and the mean orbital radii of the few lowest states in the case where the electron is confined in the interface state. These results could offer a quantitative reference for the behavior of those bound states in a more complete study of the physics of single dopants localized near an interface when the electrons tend to localize in the interface states. The theoretical model could be more realistic if the finite width of the confinement region and the image charges were taken into account. These factors can lead to a lowering of the energy levels and reducing the binding energy of the states. However, they will not alter the main feature of the energy levels and the mean orbital radius obtained here for an off-plane donor impurity. Our results within the present model are also valid for a silicon-based structure because the electrons are confined in a 2D plane. We only need to consider the in-plane effective mass (e.g. the (001) plane). Therefore, the valley coupling is not important. Our calculations were performed within the effective mass approximation. When the impurity is close to the semiconductor surface or interface ($d \approx 0$), it could introduce strain fields and modify the local electronic band structure as well as the electron effective mass. However, for a off-plane impurity, this effect would not appear and our results within the effective mass approximation are valid.

Acknowledgments

This work was supported by FAPESP and CNPq, Brazil.

Appendix. Matrix elements of the Coulomb term

By using the identity

$$\frac{1}{\sqrt{\alpha}} = \frac{2}{\sqrt{\pi}} \int_0^{+\infty} \mathrm{e}^{-\alpha u^2}\, \mathrm{d}u, \tag{A.1}$$

equation (21) takes the following form:

$$V_{n,n'}^{(m)} = -2\sqrt{\frac{2}{\pi b^2}} \int_0^{+\infty} \mathrm{e}^{-\frac{d^2}{2b^2}u^2} \left\langle R_{n,m}(\rho)|\mathrm{e}^{-\frac{\rho^2}{2b^2}u^2}|R_{n',m}(\rho)\right\rangle_\rho \mathrm{d}u. \tag{A.2}$$

Taking into account the power expansion of the associated Laguerre polynomials [26], i.e.

$$L_n^{(m)}(x) = \sum_{k=0}^{n} \binom{n+m}{n-k} \frac{(-x)^k}{k!}, \tag{A.3}$$

we obtain

$$\begin{aligned}\left\langle R_{n,m}(\rho)|\mathrm{e}^{-\frac{\rho^2}{2b^2}u^2}|R_{n',m}(\rho)\right\rangle_\rho &= \int_0^{+\infty} r_{n,m}(x) r_{n',m}(x) \\ &\times \mathrm{e}^{-\frac{x^2}{2}u^2} x\, \mathrm{d}x = Q_{n,|m|} Q_{n',|m|} \int_0^{+\infty} \left(\frac{x^2}{2}\right)^{|m|} \mathrm{e}^{-\frac{x^2}{2}(1+u^2)} \\ &\times L_n^{(|m|)}\left(\frac{x^2}{2}\right) L_{n'}^{(|m|)}\left(\frac{x^2}{2}\right) x\, \mathrm{d}x \\ &= Q_{n,|m|} Q_{n',|m|} \int_0^{+\infty} t^{|m|} \mathrm{e}^{-t(1+u^2)} L_n^{(|m|)}(t) L_{n'}^{(|m|)}(t)\, \mathrm{d}t \\ &= \sum_{s=0}^{n+n'} \frac{c_s^{(|m|,n,n')}}{(1+u^2)^{s+|m|+1}},\end{aligned} \tag{A.4}$$

with

$$Q_{n,m} = \sqrt{\frac{n!}{(n+m)!}} \tag{A.5}$$

and

$$\begin{aligned}c_s^{(m,n,n')} &= (-1)^s (m+s)! \sqrt{\frac{n!n'!}{(n+m)!(n'+m)!}} \\ &\times \sum_{k=\max(0,s-n')}^{n} \frac{1}{k!(s-k)!} \binom{n+m}{n-k} \binom{n'+m}{n'+k-s}.\end{aligned} \tag{A.6}$$

In this way, the matrix elements of the Coulomb potential are given by

$$V_{n,n'}^{(m)} = -\frac{2}{b}\sqrt{\frac{2}{\pi}} \sum_{s=0}^{n+n'} c_s^{(|m|,n,n')} I_{s+|m|}\left(\frac{d}{\sqrt{2}b}\right), \tag{A.7}$$

with

$$I_s(\alpha) = \int_0^{+\infty} \frac{\mathrm{e}^{-\alpha^2 u^2}\mathrm{d}u}{(1+u^2)^{1+s}}. \tag{A.8}$$

This integral has the following properties:

$$I_0(\alpha) = \frac{\pi}{2}\mathrm{e}^{\alpha^2}\mathrm{erfc}(\alpha), \tag{A.9}$$

$$I_1(\alpha) = \frac{\sqrt{\pi}\alpha + (1-2\alpha^2) I_0(\alpha)}{2}, \tag{A.10}$$

and

$$I_s(\alpha) = \left(1 - \frac{1}{2s} - \frac{\alpha^2}{s}\right) I_{s-1}(\alpha) + \frac{\alpha^2}{s} I_{s-2}(\alpha), \tag{A.11}$$

where

$$\mathrm{erfc}(x) = \frac{2}{\sqrt{\pi}} \int_x^{+\infty} \mathrm{e}^{-t^2}\, \mathrm{d}t \tag{A.12}$$

is the complementary error function.

By substituting (17) into (24), we obtain

$$\begin{aligned}X_{n,n'}^{(m)} &= 2 Q_{n,m} Q_{n',m} \int_0^{+\infty} \left(\frac{x^2}{2}\right)^{m+1} \mathrm{e}^{-\frac{x^2}{2}} \\ &\times L_n^{(m)}\left(\frac{x^2}{2}\right) L_{n'}^{(m)}\left(\frac{x^2}{2}\right) \mathrm{d}x \\ &= \sqrt{2} Q_{n,m} Q_{n',m} \sum_{k=0}^{n} \sum_{k'=0}^{n'} C_{k,k'}^{(m)} \binom{n+m}{n-k} \binom{n'+m}{n'-k'},\end{aligned}$$

where

$$C_{k,k'}^{(m)} = \frac{(-1)^{k+k'} \Gamma(k+k'+m+\frac{3}{2})}{k!k'!}. \tag{A.13}$$

References

[1] Kane B E 1998 *Nature* **393** 133
[2] Calderón M J, Koiller B and Sarma S D 2007 *Phys. Rev.* B **75** 125311
[3] Martins A S, Capaz R B and Koiller B 2004 *Phys. Rev.* B **69** 085320

[4] Lansbergen G P, Rahman R, Wellard C J, Woo I, Caro J, Collaert N, Biesemans S, Klimeck G, Hollenberg L C L and Rogge S 2008 *Nat. Phys.* **4** 656–61
[5] Bruno-Alfonso A, Hai G Q, Peeters F M, Yeo T, Ryu S R and McCombe B D 2001 *J. Phys.: Condens. Matter* **13** 9761–72
[6] Bruno-Alfonso A and Hai G Q 2008 *Int. J. Mod. Phys.* B **23** 3014–8
[7] Shi J M, Peeters F M and Devreese J T 1993 *Phys. Rev.* B **48** 5202–16
[8] Shi J M, Peeters F M, Hai G Q and Devreese J T 1991 *Phys. Rev.* B **44** 5692–702
[9] Hao Y L, Djotyan A P, Avetisyan A A and Peeters F M 2009 *Phys. Rev.* B **80** 035329
[10] Slachmuylders A F, Partoens B, Peeters F M and Magnus W 2008 *Appl. Phys. Lett.* **92** 083104
[11] Inoue J I, Chiba T, Natori A and Nakamura J 2009 *Phys. Rev.* B **79** 035206
[12] Kohn W and Luttinger J M 1955 *Phys. Rev.* **98** 915–22
[13] Alliluev S P 1958 *Sov. Phys.—JETP* **6** 156
[14] Zaslow B and Zandler M E 1967 *Am. J. Phys.* **35** 1118–9
[15] Cisneros A and McIntosh H V 1969 *J. Math. Phys.* **10** 277–86
[16] Parfitt D G W and Portnoi M E 2002 *J. Math. Phys.* **43** 4681–91
[17] Yang X L, Guo S H, Chan F T, Wong K W and Ching W Y 1991 *Phys. Rev.* A **43** 1186–96
[18] Yang X L, Lieber M and Chan F T 1991 *Am. J. Phys.* **59** 231–2
[19] MacDonald A H and Ritchie D S 1986 *Phys. Rev.* B **33** 8336–44
[20] Soylu A, Bayrak O and Boztosun I 2006 *Int. J. Mod. Phys.* E **15** 1263–71
[21] Robnik M and Romanovski V G 2003 *J. Phys. A: Math. Gen.* **36** 7923–51
[22] Grimaldi C 2008 *Phys. Rev.* B **77** 113308
[23] Fock V 1928 *Z. Phys.* **47** 446
[24] Darwin C 1930 *Proc. Camb. Phil. Soc.* **27** 86
[25] Faulkner R A 1969 *Phys. Rev.* **184** 713–21
[26] Gradshteyn I S and Ryzhik I M 2007 *Table of Integrals, Series, and Products* (Burlington: Academic)